

# Modelling the Flow Through a Failed Blowout Preventer

C.P. Booth<sup>1</sup>, J.W. Leggoe<sup>1</sup> and Z.M. Aman<sup>2</sup>

<sup>1</sup> Chemical Engineering Department  
University of Western Australia, Western Australia 6009, Australia

<sup>2</sup> Fluid Science and Resources Division, Chemical Engineering Department  
University of Western Australia, Western Australia 6009, Australia

## Abstract

Predicting the droplet sizes produced by a jet is important in fields ranging from the pharmaceutical industry to emergency planning in the event of a deep-sea well blowout. Current scaling models are usually based on experimental results obtained using a straight pipe entering a quiescent media. As the process of breakup is governed by the local turbulent fields, the history of the jet fluid upstream from the entry to the quiescent domain is important. Turbulence generated by the extreme shear gradients arising at obstruction within the pipe will be advected a significant distance downstream, including beyond the jet exit. This work shows that an orifice plate inserted into a pipe upstream of the exit alters the jet that emerges, even when the orifice plate is a several diameters upstream of the opening. The effect in general is to enhance the spreading of the jet due to the influence of the turbulence kinetic energy generated at the orifice plate that has been transported into the exiting jet.

## Introduction

The Macondo Blowout in April 2010 released approximately 780,000 cubic metres of oil and gas into the Gulf of Mexico [2]. The fate of the released oil is determined by the droplet sizes formed. The larger droplets rapidly rise to the surface, while the smaller droplets can become trapped in inversion layers (and then transported by sub-surface currents in potentially different directions than the surface currents and wave action that transport the surfaced oil) [3]. As the emergency response needs to take this into account, knowing the droplet size distribution (DSD) is important. Experiments to determine the DSD from a full scale event are not practicable, so current work has been based on lab scale vertical jets [4], horizontal jets [5], and autoclave experiments [6], all of which have been used to calibrate scaling laws. A potential downside of these experiments, in the case of the jets, is the assumption that the flow creating the jet can be approximated accurately as a fully developed pipe flow.

In the Macondo Blowout, when the Blowout Preventer (BOP) was activated it failed to seal-in the well and severed the drill pipe. This meant that fluids could now flow through the annular space as well the drill pipe. Before the riser was severed on June 3, the flow geometry from the wellhead to the environment was complicated by a number of tears and kinks in the riser, which allowed oil and gas to escape into the ocean in addition to the flow from the severed end of the riser and drill pipe [7]. After the riser was severed the flow of the fluids into the environment was complicated by the remains of the drill string, along with the failed and closed rams and preventers inside the BOP stack. The topmost of these was the Upper Annular Preventer (UAP) seen in Figure 1 [1]. This work looks at the effect that obstructions inside the BOP, such as the UAP, could have on the jet from the severed riser, by considering systems in which a single orifice plate obstruction has been introduced upstream of the jet exit.



Figure 1. Photo of the upper annular preventer recovered from the Macondo BOP stack after it was sealed [1].

## Method & Results

The simulations presented in this paper used the finite-volume based CFD software ANSYS FLUENT® version 18.2. Axisymmetric models were created in which the SST- $\omega$  Turbulence Model with Low Reynolds Number correction was employed, due to its ability to accurately capture the near-wall dynamics of pipe flow. The discretisation of the momentum and turbulence equations used the 3<sup>rd</sup> Order MUSCL method, and pressure the 2<sup>nd</sup> Order method. The inlet boundary condition to the pipe for both models consisted of fully developed velocity,  $k$ , and  $\omega$  profiles obtained from a periodic pipe simulation. To validate the turbulence model the simulation of an orifice plate was compared against the experimental work of Shan, et al. [8] where the location of the vena contracta and reattachment points for the system are reported. Shan et al's pipe diameter was 46mm, the orifice plate was 5mm thick and had a beta ratio ( $D_{\text{orifice}}/D_{\text{pipe}}$ ) of 0.5, the working fluid was water and the velocity was set to have an orifice/pipe based Reynolds number of 25000. To ensure that the discretisation error was minimised a mesh convergence study was conducted, details of which are given in Table 1. As the wall effects are important, the meshes were designed so that wall  $y^+$  was always less than 1. As the difference between meshes O2 and O3 was less than 2% the mesh was considered converged and the bulk size of 0.5mm from mesh O3 was used for the free jet simulations. For the mesh O3 the wall  $y^+$  varied between 0.003 to 0.59.

	Elements	Max TKE [J/kg]	% Difference
O1	21,225	$3.608 \times 10^{-3}$	
O2	44,490	$3.355 \times 10^{-3}$	7.54
O3	124,680	$3.294 \times 10^{-3}$	1.85

Table 1. Results from the mesh convergence study, showing the maximum TKE on the pipe axis.

	Vena Contracta	Reattachment Length
Experimental	27.6 mm	109 mm
Simulation	32.3 mm	161 mm
Difference	17%	47.7%

Table 2. Comparison of the results from the experiments of Shan et al [8] with simulations. The location of the vena contracta and reattachment are given as the distance from the exit of the orifice plate.

The jet simulations used the same settings as the orifice plate simulations, with the physical dimensions of the model domain given in figure 2. A block structured mesh was generated on the region inside the pipe and immediately after the pipe exit after which a quadrilateral dominated mesh was used to fill the simulation domain. The orifice plate was placed at several locations to observe the effect this had on the jet that formed. Two simulations had no orifice plate with one having a reduced diameter of 23mm, the others were chosen to be 0, 55, 161, 255, and 355mm (0, 2D<sub>o</sub>, 7D<sub>o</sub>, 11D<sub>o</sub>, 15.4D<sub>o</sub>) upstream of the exit. The simulation with the plate at 161mm is noted with (RA), as this was equivalent to the reattachment length for the validation simulation (orifice plate flow in pipe), and it was expected that different regimes would be observed based on whether the jet reattached before it leaves the pipe.

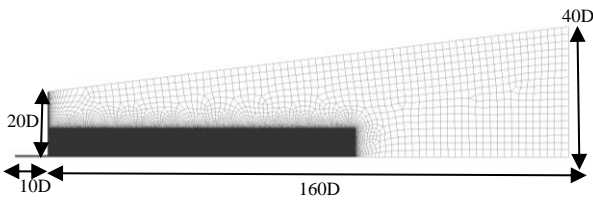


Figure 2: Mesh overview showing high resolution area around the pipe and jet area and the lengths of the geometry with respect to the inlet pipe diameter (D = 46mm)

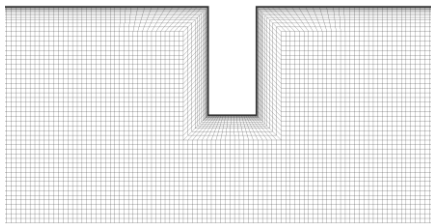


Figure 3: Zoomed in section of mesh around the orifice plate.

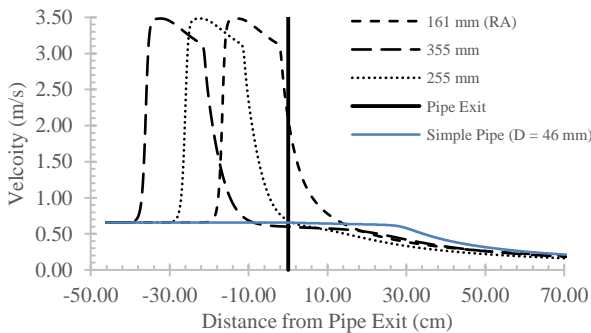


Figure 4: Plot of velocity magnitude along the pipe/jet centreline for the three simulations where the orifice plate flow reattached before exiting the pipeline. The vertical black line represents the location of the pipe exit.

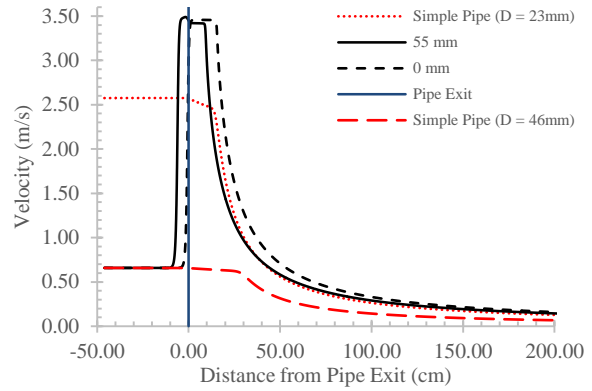


Figure 5: Plot of velocity magnitude along the pipe/jet centreline comparing results when the orifice plate was placed so that the orifice plate flow doesn't reattach before exiting the pipe with a pipe simulation having no orifice plate and a diameter equal to the internal diameter of the orifice plate. The vertical blue line represents the location of the pipe exit.

Figure 4 shows the centreline velocity magnitudes for three simulations where the orifice plate was positioned so that the orifice plate flow reattaches before it exiting the pipe. It can be seen that due to the increase in turbulent kinetic energy, the jet expands quicker than it would without the plate (as evident in the reduced centreline velocities). In Figure 5 it can be seen when the orifice plate is placed such that the internal jet doesn't reattach before exiting the pipe the dynamics are significantly altered. It can also be seen that simply modifying the inlet pipe to match the diameter of the upstream orifice plate doesn't capture the flow field behaviour. In part this is due to the throat of the orifice plate being short enough that satisfying the momentum balance equations causes the flow to contract to be narrower than the orifice diameter.

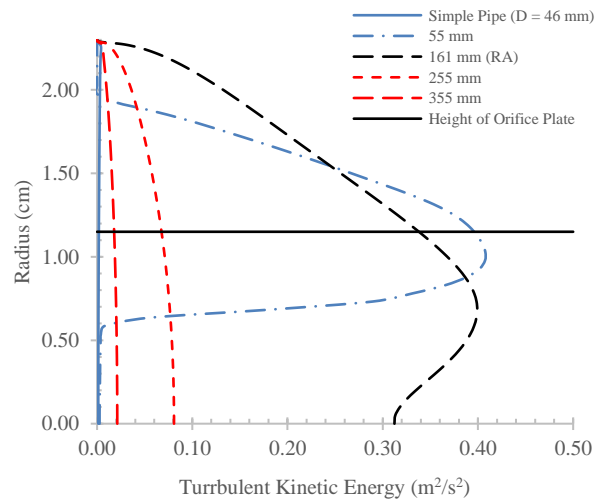


Figure 6: Profiles of the Turbulent Kinetic Energy at the pipe exit for the simulation with no orifice plate and the simulations where an orifice plate is placed inside the pipe. The solid black line represents the radius of the orifice plate

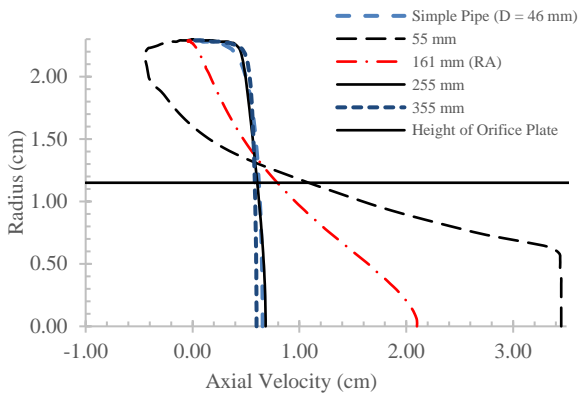


Figure 7: Profiles of the axial velocity at the exit of the pipe for some simulations. The horizontal black line represents the radius of the orifice plate.

Figures 6 and 7 show the turbulent kinetic energy (TKE) and axial velocity profiles at the exit of the pipe. When the orifice plate flow reattaches before exit, the axial velocity profiles at the exit resemble that for a simple pipe flow. However, the TKE profiles exhibit a pronounced increase in TKE even when the flow has reattached. In other words, even though the velocity profile has re-established, the significant turbulence generated at the orifice plate is advected downstream to the exit, and has not been dissipated. This leads to the centreline velocity behaviour seen in Figure 4, as the additional turbulence causes the jet to spread laterally more rapidly beyond the pipe exit.

In the simulations where the jet was either just beginning to or was unable to reattach, the TKE and velocity profiles have a completely different structure. The axial velocity profile for the simulation where the plate is 55mm away from the exit exhibits strong recirculation region at the exit, along with the flattened velocity profile near the centre of the pipe. These profiles suggest that experimental investigations would need to strongly condition the flow to simulate the effect of upstream restrictions on jet dynamics.

As jet breakup is a local process the turbulent dissipation rate (TDR) is also used to approximate the energy that will go into breaking up droplets. In Figures 9 and 10 the TDR for the simple pipe jet (with no orifice plate) and the simulation with the orifice plate at 161mm upstream are plotted for the region just outside the pipe exit. The peak TDR of  $0.6 \text{ m}^2/\text{s}^3$  for the simple pipe jet occurs in the boundary layer near the exit, while for the simulation with the plate 161mm upstream of the exit the peak of  $183 \text{ m}^2/\text{s}^3$  occurs in the internal jet that forms at the orifice plate. The increased TDR is transported downstream into the quiescent domain and spans a significantly larger region; this is critical for multiphase jets, as jet break up will take place beyond the pipe exit.

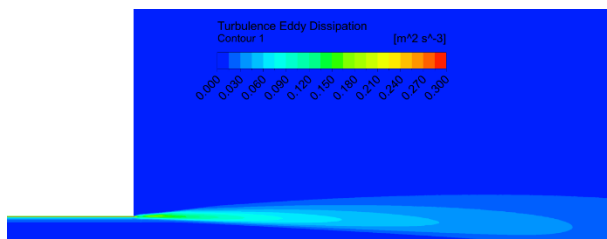


Figure 9: Contours of TDR near the exit for the simple pipe jet. The legend has been rescaled to better visualise the TDR after the exit with a real peak of  $0.6 \text{ m}^2/\text{s}^3$ .

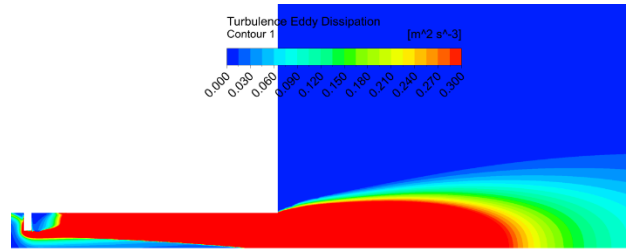


Figure 10: Contours of TDR for the 161mm simulation using the same contour scale as figure 9. Note that the true peak TDR for this simulation was  $183 \text{ m}^2/\text{s}^3$ , nearly 3 orders of magnitude greater than that in the simple pipe simulation presented in figure 9.

While this work demonstrates the influence of flow history on the behaviour of jets, the assumption of single-phase axisymmetric flow doesn't capture the complexities seen in the Macondo Blowout event. In particular, this model is missing the effect of the damaged Blind Shear Ram which lay below (upstream of) the UAP, and would be another significant generator of turbulence. Similarly, the pinches and tears to the riser and Lower Marine Riser Package can't be captured. All of these geometric changes would change the flow of the jet to some extent, and their effect on the free jet and the droplet size distribution will need to be quantified.

## Conclusions

In this work we have shown that the upstream history of a turbulent jet is important, as the turbulence generated by obstructions in the flow upstream of the exit into the quiescent medium will be advected to the exit and beyond into the medium. Even when the internal jet generated by an orifice plate reattaches before exit, the increase in turbulent kinetic energy is advected into the free jet, leading to the jet spreading faster than without an obstruction. When the internal jet orifice plate is unable to reattach before exiting, the jet carries its narrowed profile and elevated turbulence into the free domain, leading to jet with a narrower initial profile but dramatically enhanced spreading and break-up potential.

The profile of the jet at the exit for the reattached jets is similar to that of a simple pipe jet, but with an increased TKE, meaning that that the incoming flow should be conditioned to capture the effects of any upstream obstruction in experimental work. When the jet doesn't reattach, the exit profile has an entirely different profile including a recirculation region and a TKE peak towards the centre of the flow field, again suggesting that the any experimental flow would need to strongly conditioned to simulate the obstruction. These simulations have shown that simply replacing the pipe with one equivalent to the effective diameter of the obstruction will not be sufficient to capture the true behaviour.

## References

- [1] Det Norske Veritas, "Forensic Examination of Deepwater Horizon Blowout Preventer, Vols. I and II "in" Final Report for U.S. Department of the Interior, Bureau of Ocean Energy Management, Regulation, and Enforcement," Washington, D.C.2011, vol. Report No. EP030842. Available: <https://www.bsee.gov/sites/bsee.gov/files/research-guidance-manuals-or-best-practices/regulations-and-guidance/dnvreportvolumeii.pdf>
- [2] S. K. Griffiths, "Oil Release from Macondo Well MC252 Following the Deepwater Horizon Accident,"

*Environmental Science & Technology*, vol. 46, no. 10, pp. 5616-5622, 2012.

- [3] C. B. Paris et al., "Evolution of the Macondo Well Blowout: Simulating the Effects of the Circulation and Synthetic Dispersants on the Subsea Oil Transport," *Environmental Science & Technology*, vol. 46, no. 24, pp. 13293-13302, 2012.
- [4] Ø. Johansen, P. J. Brandvik, and U. Farooq, "Droplet breakup in subsea oil releases – Part 2: Predictions of droplet size distributions with and without injection of chemical dispersants," *Marine Pollution Bulletin*, vol. 73, no. 1, pp. 327-335, 2013.
- [5] L. Zhao *et al.*, "Underwater oil jet: Hydrodynamics and droplet size distribution," *Chemical Engineering Journal*, vol. 299, pp. 292-303, 2016.
- [6]
- [7] Z. M. Aman, C. B. Paris, E. F. May, M. L. Johns, and D. Lindo-Atichati, "High-pressure visual experimental studies of oil-in-water dispersion droplet size," *Chemical Engineering Science*, vol. 127, pp. 392-400, 2015.
- [8] M. K. McNutt *et al.*, "Review of flow rate estimates of the Deepwater Horizon oil spill," *Proceedings of the National Academy of Sciences*, vol. 109, no. 50, pp. 20260-20267, 2012.
- [9] F. Shan, Z. Liu, W. Liu, and Y. Tsuji, "Effects of the orifice to pipe diameter ratio on orifice flows," *Chemical Engineering Science*, vol. 152, pp. 497-506